Universität des Saarlandes

Fachrichtung 6.1 – Mathematik

Preprint

Multifrequency Analysis for the Helmholtz Equation

Mirjam Köhl and Sergej Rjasanow

Preprint No. 64

Saarbrücken 2002

Universität des Saarlandes

Fachrichtung 6.1 – Mathematik

Multifrequency Analysis for the Helmholtz Equation

Mirjam Köhl

Saarland University
Department of Mathematics
Postfach 15 11 50
D–66041 Saarbrücken
Germany
E-Mail: koehl@num.uni-sb.de

Sergej Rjasanow

Saarland University
Department of Mathematics
Postfach 15 11 50
D–66041 Saarbrücken
Germany
E-Mail: rjasanow@num.uni-sb.de

submitted: June 26, 2002

Preprint No. 64

Saarbrücken 2002

Edited by
FR 6.1 – Mathematik
Im Stadtwald
D–66041 Saarbrücken
Germany

Fax: + 49 681 302 4443
e-mail: preprint@math.uni-sb.de
WWW: http://www.math.uni-sb.de/

Abstract

In this paper a new numerical method for the multifrequency analysis of the three-dimensional Helmholtz equation is introduced. The Collocation Boundary Element Method (BEM) is used for the discretisation of the problem. The identity of the Fourier transform with respect to the wave number is applied to the matrix of the resulting linear system. The analytical form and some important properties are derived. Some numerical examples for the solution are presented.

AMS Subject Classification:
Key words: collocation methods, Helmholtz equation, Fourier transform

Contents

1 Introduction

An important assignment for engineers who design electro-magnetic components for automobiles is the reduction of the noise which results from acoustic radiation emitted by the surfaces of these vibrating components.
The mathematical model of this technical problem can be represented by a three-dimensional exterior boundary value problem for the Helmholtz equation. The associated boundary integral equation (BIE) is formulated in terms of the surfaces of the components, so one of the most complicated problems is the numerical solution for the BIE. The boundary element method (BEM)

produces large dense matrices especially for complex, practically relevant geometries in 3D, where a large number of panels is needed to obtain a sufficiently accurate approximation of the boundary. The memory requirement is $Mem = O(N^2)$ and the numerical work using classical direct solvers is given by $Op = O(M\,N^3)$ where M denotes the number of frequencies and N is the number of degrees of freedom. Engineers are interested in a wide spectrum of frequencies $\nu \in [0, \nu_{max}]$.
Typical values are $N = 10^3 - 10^4$ for the dimension of the problem and $M = 10^1 - 10^2$ for the frequencies of interest.
In this paper, we introduce a new method for the multifrequency analysis of the Helmholtz equation which is based on the Fourier transform with respect to the wave number κ (and so the frequency).

The paper is organised as follows. In Section 2 we give a short description of the exterior boundary value problem for the Helmholtz equation and its properties. The boundary integral formulation of the problem and the discrete form are the topics of Sections 3 and 4. In Section 5 we give a short review of the Fourier transform and its main properties. We present, in Section 6, the new system of collocation equations after applying the Fourier transform. Finally, we give some numerical examples, Section 7, and some conclusions, Section 8.

2 The Helmholtz Equation

We consider the exterior boundary value problem for the three-dimensional Helmholtz equation [2]

$$\begin{aligned} \Delta\, u(x) + \kappa^2 u(x) &= 0\,,\ x \in \mathbb{R}^3 \setminus \Omega\,, \\ l(u(x)) &= g(x)\,,\ x \in \Gamma\,. \end{aligned} \tag{1}$$

In (1) κ is the wave number which may be real or complex with $Im\,(\kappa) \geq 0$. $\Gamma = \partial\Omega$ denotes the boundary of the bounded domain Ω and $g(x)$ is a given function. l is a boundary operator corresponding to the Dirichlet, Neumann or impedance boundary condition on Γ.
Here, we restrict our discussion to the case of the Dirichlet problem

$$u(x) = g(x)\,,\ x \in \Gamma\,. \tag{2}$$

To quarantee uniqueness of the solution $u(x)$, we add the Sommerfeld radiation conditions or outgoing wave conditions [6]

$$\Big(\frac{\partial}{\partial r} - i\kappa\Big) u(x) = o\,(\,|x|^{-1}) \text{ and } u(x) = O\,(\,|x|^{-1}) \quad \text{for large } |x| = r\,. \tag{3}$$

Notice that the fundamental solution of the Helmholtz equation is known

$$\Delta u^*(x,y,\kappa) + \kappa^2 u^*(x,y,\kappa) = -\delta(x-y)$$

where for $x, y \in \mathbb{R}^3$

$$u^*(x,y,\kappa) = \frac{1}{4\pi}\frac{e^{i\kappa|x-y|}}{|x-y|}\,. \tag{4}$$

It should be pointed out that the fundamental solution (4) satisfies the Sommerfeld radiation conditions [1].

3 Boundary Integral Formulation

The boundary integral equations for the exterior Dirichlet boundary value problem in (1) will be reviewed, according to [2].
For a given density function $f(\cdot,\kappa)$ defined on Γ and $y \in \mathbb{R}^3$, we let

$$V_1(f)(y,\kappa) = \int_\Gamma u^*(x,y,\kappa) f(x,\kappa)\, dF_x \tag{5}$$

$$V_2(f)(y,\kappa) = \int_\Gamma \frac{\partial\, u^*(x,y,\kappa)}{\partial\, n_x} f(x,\kappa)\, dF_x \tag{6}$$

be the single- and double-layer potentials for the Helmholtz equation.
Note that both potentials satisfy the Sommerfeld radiation conditions (3).

Using the single-layer potential V_1 in (5), to treat the Dirichlet BVP, we would need to solve the boundary integral equation for $y \in \Gamma$

$$\mathcal{A}f(y,\kappa) \equiv \int_\Gamma u^*(x,y,\kappa) f(x,\kappa)\, dF_x = g(y,\kappa)\,, \tag{7}$$

where f is the single-layer density representing the solution of (1).

We now give a uniqueness theorem for the solution.

Theorem 1 *The exterior Dirichlet BVP*

$$\begin{aligned} &\Delta u(y) + \kappa^2 u(y) = 0 \qquad \textit{for } y \in \Omega^c \\ &u(y) = g(y) \in H^r(\partial\Omega) \quad \textit{for } y \in \partial\Omega\,, \quad r \in \mathbb{R} \\ &u \textit{ satisfies the radiation conditions } (3) \end{aligned} \tag{8}$$

has a unique solution

$$u(y) = \int_\Gamma u^*(x,y,\kappa) f(x,\kappa)\, dF_x \in H^{r+\frac{3}{2}}_{loc}(\Omega^c) \tag{9}$$

for a unique $f \in H^r(\partial\Omega)$ solving the BIE (7), provided $-\kappa^2$ is not an eigenvalue of the interior Dirichlet BVP for the Laplacian.

Remark 2 *If $-\kappa^2$ is an eigenvalue of the interior Dirichlet BVP for the Laplacian, then the BIE (7) is solvable if and only if g is orthogonal to the cokernel (=kernel) of $\mathcal{A}$. In this case, the solution f is not unique, cf. [3].*

In a similar manner we can use the double-layer or the combined single- and double-layer representations to solve the exterior Dirichlet BVP.
The associated uniqueness theorems for all wave numbers κ are given in [2].

Throughout the rest of this discussion, we assume that $\kappa \in \mathbb{R}^+$.
Restricting our discussion to the case of the single-layer representation, we assume that the equation (7) is solvable.

4 Collocation Method

The numerical solution for the equation (7) begins with the discretisation of the surface Γ using a system of plane, triangle panels

$$\Gamma \approx \Gamma_h = \bigcup_{j=1}^{N} \Gamma_j \,.$$

The centres of the mass of the panels Γ_i build a system of collocation points y_i

$$y_i = \frac{1}{3}\left(x_i^{(1)} + x_i^{(2)} + x_i^{(3)}\right), \quad i = 1, \ldots, N \,.$$

Let the unknown function $f(x,\kappa)$ on Γ be approximated by

$$f_h(x,\kappa) = \sum_{j=1}^{N} \alpha_j(\kappa)\varphi_j(x)$$

where φ_j is piecewise constant on Γ_j:

$$\varphi_j(x) = \begin{cases} 1 \text{ on } \Gamma_j \\ 0 \text{ otherwise.} \end{cases}$$

Thus we obtain the following system of collocation equations

$$A(\kappa)\alpha(\kappa) = b(\kappa)\,,\ A \in \mathbb{C}^{N\times N}\,,\ \alpha,\, b \in \mathbb{C}^N \tag{10}$$

where the elements of the matrix A are defined as

$$a_{ij}(\kappa) = \frac{1}{4\pi}\int\limits_{\Gamma} \frac{e^{i\kappa|x-y_i|}}{|x-y_i|}\varphi_j(x)dF_x\,. \tag{11}$$

The vector α and the right-hand side of this system are given by

$$(\alpha(\kappa))_j = \alpha_j(\kappa) \text{ and } (b(\kappa))_i = g(y_i,\kappa)\,,\quad i,j = 1,\ldots,N\,.$$

Note that the equation (10) explicitly depends on the wave number κ.

5 Fourier Transform

In this section we give some basic definitions and properties of the Fourier transform for our subsequent applications. For more details we refer the reader to [2], [5] .
For a complex-valued function f on $\mathbb{R}$, we define the one-dimensional Fourier transform of f by

$$\hat{f}(\kappa) \equiv \mathcal{F}_{\xi,\kappa}[f(\xi)](\kappa) = \int\limits_{\mathbb{R}} f(\xi)e^{i\kappa\xi}d\xi \quad ,\kappa \in \mathbb{R}\,. \tag{12}$$

The corresponding inverse Fourier transform is then

$$f(\xi) = \mathcal{F}^{-1}_{\kappa,\xi}[\hat{f}(\kappa)](\xi) = \frac{1}{2\pi}\int\limits_{\mathbb{R}} \hat{f}(\kappa)e^{-i\kappa\xi}d\kappa\,, \tag{13}$$

from which we also have

$$\check{f}(\xi) \equiv \mathcal{F}^{-1}_{\kappa,\xi}[f](\xi) = \frac{1}{2\pi}\hat{f}(-\kappa) \quad \text{resp.} \quad \mathcal{F}_{\xi,\kappa}[\hat{f}](\kappa) = 2\pi f(-\kappa)\,. \tag{14}$$

The Fourier transform $\hat{f}$ exists, at least, for $f \in \mathbb{L}_1$. In particular, (12) and (13) define the Fourier transform and its inverse for every test function $f \in \mathbb{S}$. It is well known that the Schwartz space $\mathbb{S}$ is invariant under the Fourier transform and that under its inverse

$$\mathcal{F}^{\pm 1} : \mathbb{S} \to \mathbb{S}\,.$$

An important property of the Fourier transform is given by the Bessel-Parseval formula

$$\langle f, g\rangle_{\mathbb{L}_2} = \int_{\mathbb{R}} f(\kappa)\overline{g(\kappa)}d\kappa = \frac{1}{2\pi}\langle \hat{f}, \hat{g}\rangle_{\mathbb{L}_2} \quad \text{for all } f, g \in \mathbb{L}_2\,.$$

We notice that the Fourier transform of a tempered distribution $\psi \in \mathbb{S}'$ is defined by

$$\langle \psi, \hat{f}\rangle = \langle \hat{\psi}, f\rangle$$

which holds for every test function $f \in \mathbb{S}$ and has the property

$$\mathcal{F}^{\pm 1} : \mathbb{S}' \to \mathbb{S}'.$$

Later we will need the inverse Fourier transform of the constant 1.
Since the Fourier transform of the even Dirac δ-distribution is known

$$\hat{\delta} = 1$$

we get, through (14),

$$\hat{1} = \hat{\hat{\delta}}(x) = \delta(x) \quad \text{and} \quad \check{1} = \delta(x)\,. \tag{15}$$

6 New Linear System

Applying the identity of the Fourier transform with respect to the wave number κ to the collocation matrix (11) we obtain

$$A(\kappa) = \mathcal{F}_{\xi,\kappa}\left[\mathcal{F}^{-1}_{\kappa,\xi}\left[\,A(\kappa)\,\right](\xi)\right](\kappa)\,. \tag{16}$$

The entries of the matrix $\check{A}(\xi) = \mathcal{F}^{-1}_{\eta,\xi}\left[\,A(\eta)\,\right](\xi)$ are given by

$$\begin{aligned}\check{a}_{ij}(\xi) &= \frac{1}{2\pi}\int_{\mathbb{R}} a_{ij}(\kappa)e^{-i\kappa\xi}d\kappa \\ &= \frac{1}{4\pi}\frac{1}{\xi}\int_{\Gamma} \delta(\xi - |x - y_i|)\varphi_j(x)dF_x \end{aligned} \tag{17}$$

as a consequence of

$$\mathcal{F}^{-1}_{\kappa,\xi}[e^{i\kappa|x-y_i|}](\xi) = \mathcal{F}^{-1}_{\kappa,\xi}[1](\xi - |x - y_i|) \tag{18}$$

and (15).

Remark 3 *The Dirac δ-distribution in (17) describes a ball of radius ξ centred at y_i.*
Due to its definition the integration domain leads to integration over the intersection of Γ and the surface of the ball.
Note that ξ is reduced to $[\,0, diam(\Gamma)\,]$ where $diam(\Gamma) = \sup_{x,y\in\Gamma} |x-y|$.

If we assume that Γ_j, $j = 1, \ldots, N$, are plane triangles then the corresponding elements of the matrix $\check{A}(\xi)$ can be computed analytically in the following way.
Let us denote the projection of the point y_i into the plane of the triangle Γ_j with y_i', $\quad y_i' = y_i - d \cdot n_j$. First we rotate and translate the system of coordinates in such a way that the origin coincides with the point y_i', the e_1-axis is directed along a side of the triangle, especially the side $x_j^{(1)} x_j^{(2)}$, and the e_3-axis is directed along the unit normal vector n_j. In these new coordinates a point $x \in \Gamma_i$ takes the form

$$x' = Q(x - y_i') = (x_1', x_2', 0)$$

where Q denotes the corresponding rotation matrix.
Figure 1 illustrates the situation described.

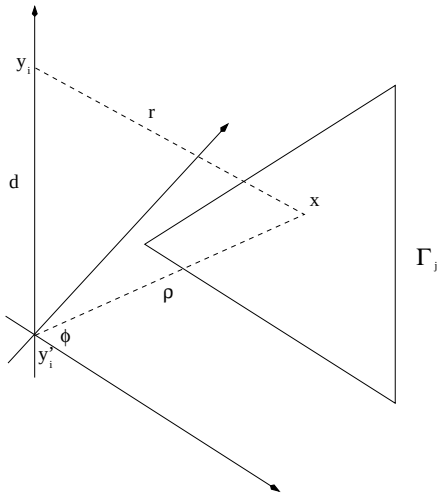

Figure 1: Computation of the elements of the matrix

The integral in (17) will be evaluated in polar coordinates in the plane of the triangle Γ_j. Using the notation from Figure 1 and noting that $\varrho d\varrho = r dr$ we obtain

$$\check{a}_{ij}(\xi) = \frac{1}{4\pi}\frac{1}{\xi}\int_{\Phi_1}^{\Phi_2}\int_{d}^{r_{max}} \delta(\xi - r)\varphi_j(x(r,\Phi)) r dr d\varphi = \frac{1}{4\pi}\left(\Phi_2(\xi) - \Phi_1(\xi)\right)\,, \quad (19)$$

$i, j = 1, \ldots, N$, since $\varphi_j(x)$ is piecewise constant on Γ_j.

Notice that each element $\check{a}_{ij}(\xi)$ has a local support, $\text{supp}[\,\check{a}_{ij}\,] = [\xi_{min}, \xi_{max}\,]$, cf. Remark 3. Therefore the matrix $\check{A}(\xi)$ is real and has a sparse structure for a fixed ξ.

In order to solve the system of linear equations (10) we need to examine the Fourier transform of the matrix $\check{A}(\xi)$ (cf. (16)).
Since each element $\check{a}_{ij}(\xi)$ has a local support we can restrict the integration domain to the support of the element.
Inside this interval the function will be approximated using a set of m piecewise constant splines and we obtain the following relations for the entries of $A(\kappa)$

$$\int_{\mathbb{R}} \check{a}_{ij}(\xi) e^{i\kappa\xi} d\xi \approx h_\xi \sum_{l=0}^{m-1} \check{a}_{ij}(l) \int_{l}^{l+1} e^{i\kappa(\xi_{min}+th_\xi)} dt\,.$$

where

$$\check{a}_{ij}(l) = \int_{l}^{l+1} \check{a}_{ij}(\xi_{min} + th_\xi) dt \quad \text{and} \quad h_\xi = \frac{\xi_{max} - \xi_{min}}{m}\,,\ m \in \mathbb{N}.$$

A short calculation of the integral term leads to the new linear system

$$\tilde{A}(\kappa)\alpha(\kappa) = b(\kappa)\,,\ \tilde{A} \in \mathbb{C}^{N\times N}\,,\ \alpha,\, b \in \mathbb{C}^N \tag{20}$$

where the elements of the matrix $\tilde{A}$ are defined as

$$\tilde{a}_{ij}(\kappa) = h_\xi\, e^{i\kappa(\xi_{min}+\frac{h_\xi}{2})}\, \text{sinc}\left(\frac{\kappa h_\xi}{2}\right) \sum_{l=0}^{m-1} \check{a}_{ij}(l) e^{i\kappa l h_\xi}\,. \tag{21}$$

Since the term outside the sum depends only on the wave number κ the sum will be estimated separately.
A further property is that the values $\check{a}_{ij}(l)$ are independent of the choice of wave number. This allows us to treat the linear system for several $\kappa \leq L$ using the same data $\check{a}_{ij}(l)$ for each of them.
Remember that L corresponds to the highest frequency

$$L = 2\pi \frac{\nu_{max}}{c}$$

where c is the velocity.

It should be remarked that we can analytically compute the entries of the double-layer potential matrix in a similar manner.

7 Numerical Results

We consider the surface of the unit sphere

$$\Gamma = \{x \in \mathbb{R}^3, |x| = 1\},$$

approximated using a system of $N = 1280$ plane, triangle panels.
The maximal wave number is given by $L = 8$ and we are interested in $M = 200$ frequencies.

The following numerical tests were performed for the boundary integral equation

$$\mathcal{A}v = \left(\frac{1}{2}\mathcal{I} + \mathcal{B}\right) f \quad \text{and} \quad \mathcal{A}v = \left(-\frac{1}{2}\mathcal{I} + \mathcal{B}\right) f \tag{22}$$

of the respective interior and exterior Dirichlet BVPs of the Helmholtz equation using collocation with piecewise constant ansatz functions.
In the above $\mathcal{A}$ and $\mathcal{B}$ denote the single-layer and double-layer potentials of the Helmholtz equation.

Since we chose

$$f = u^*(x, y_o, \kappa) = \frac{1}{4\pi}\frac{e^{i\kappa|x-y_o|}}{|x-y_o|}, \quad x \in \Gamma,$$

$y_o \notin \overline{\Omega}$ for the interior and $y_o \in \Omega$ for the exterior problem, the solution of the equation (22) is known to be $v = \partial_{n_x} u^*(x, y_o, \kappa)|_{x\in\Gamma}$.

In order to examine the behaviour of the solutions which arise from the Fourier method v_{FT}, we compare these and the results using standard techniques v_{ST} with the analytical solutions v. Note that we use numerical integration for the computation of the matrices in the case of v_{ST}.
In the graphs below the solution v_{FT} is highlighted in black, v_{ST} is pointed and the dashed line corresponds to the analytical solution.

Figure 2 shows the error of the solutions in the $\mathbb{L}_2$ norm. The error of the solution using the Fourier method is almost constant except for the discrete peaks, whereas the error of v_{ST} increases with a larger wave number. The peaks result from the fact that the negative square of these wave numbers are exactly the eigenvalues of the Laplacian on the unit sphere.

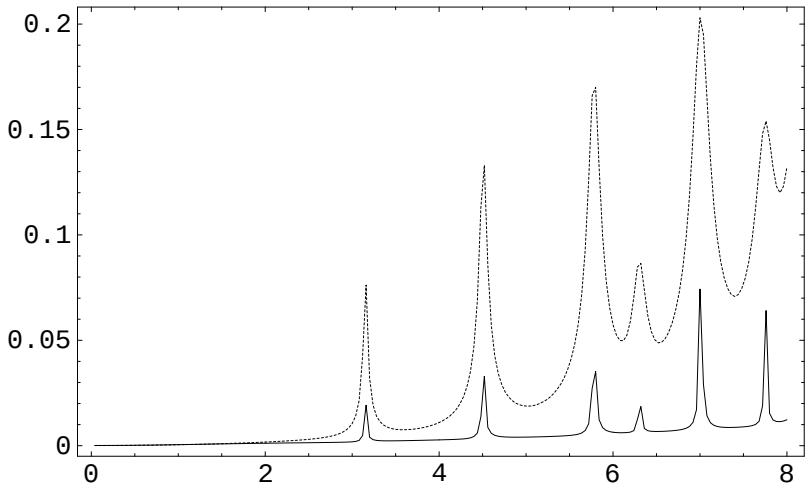

a) Interior Problem

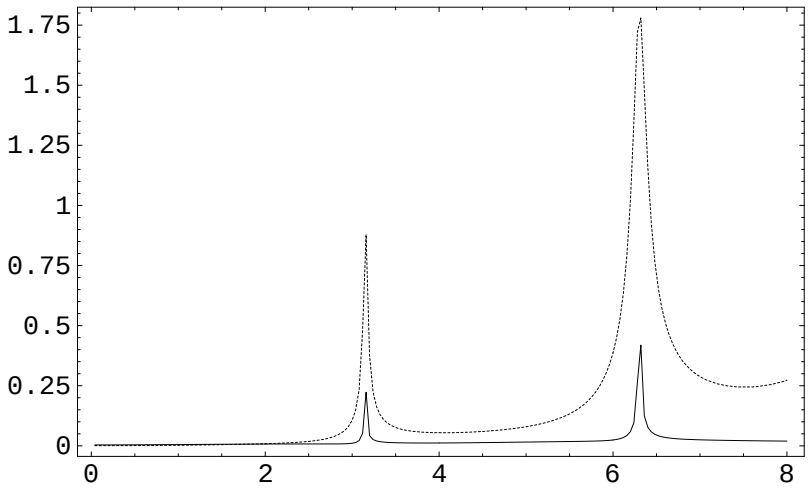

b) Exterior Problem

Figure 2: $\mathbb{L}_2$ error of the solutions in dependence on the wave number

The course of one component of the solutions depending on the wave number is presented in Figures 3 and 4. In both cases, the Fourier method provides results which coincide well with the analytical values. The curve of the solution using standard techniques differs increasingly for larger wave numbers.

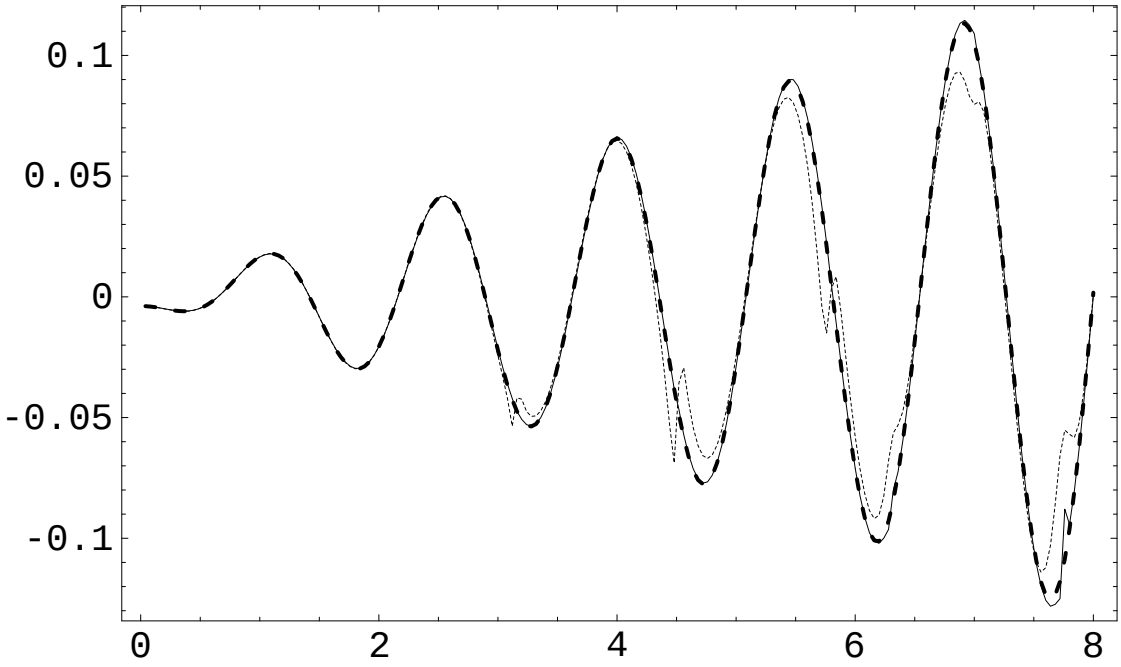

a) Real Part

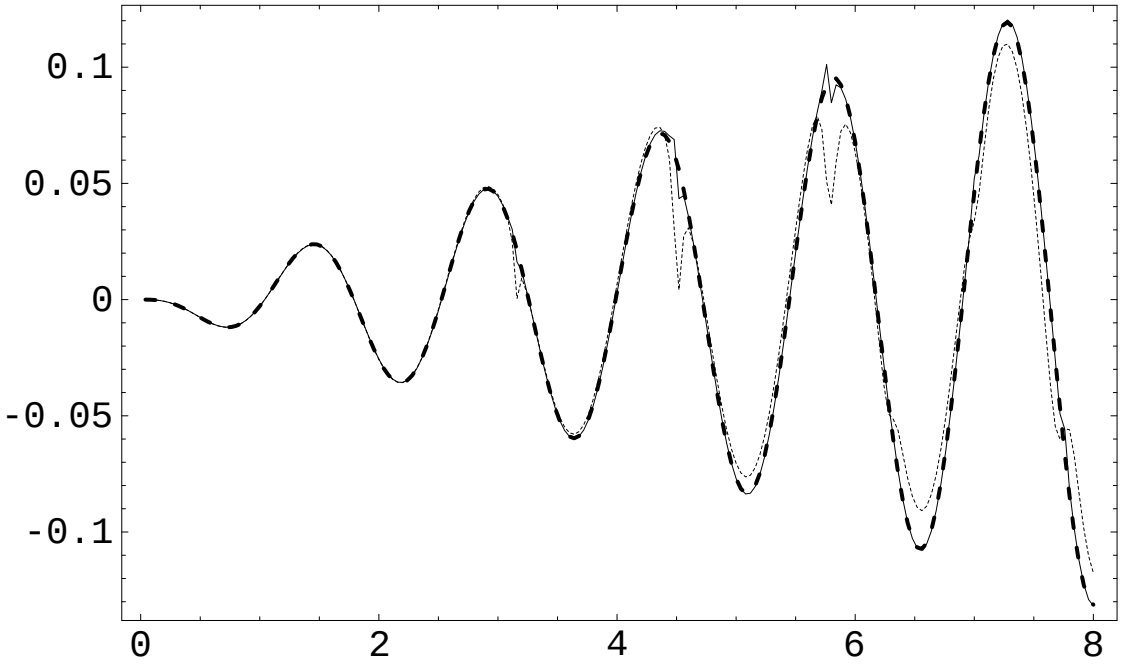

b) Imaginary Part

Figure 3: The course of the solutions in dependence on the wave number - Interior problem

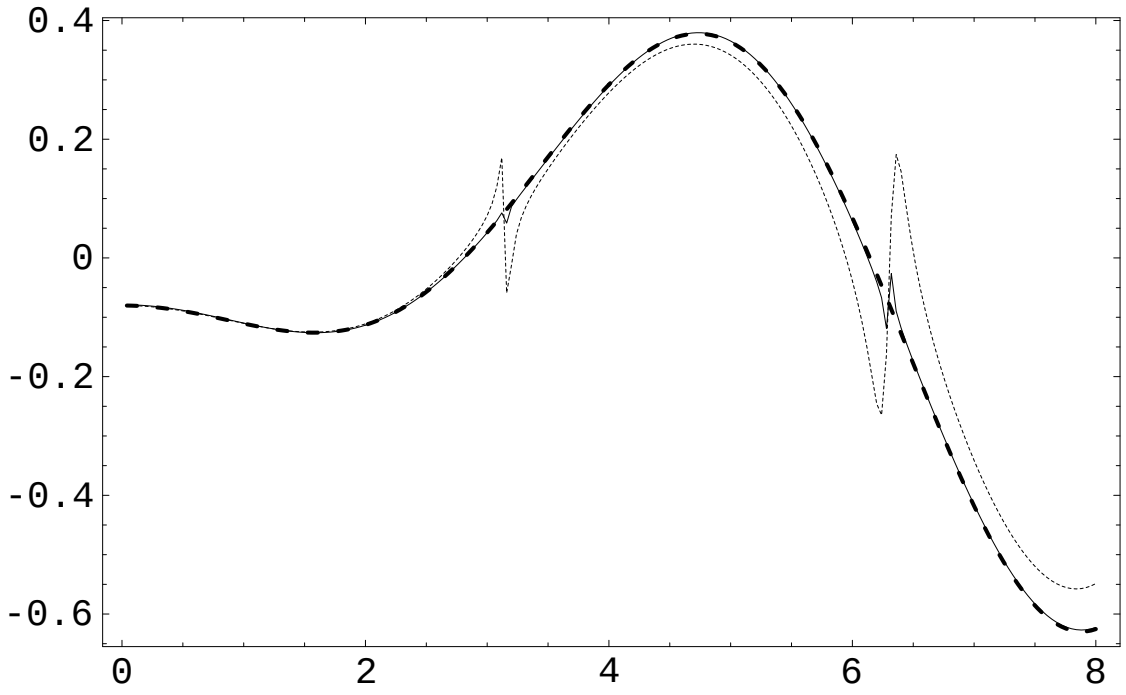

a) Real Part

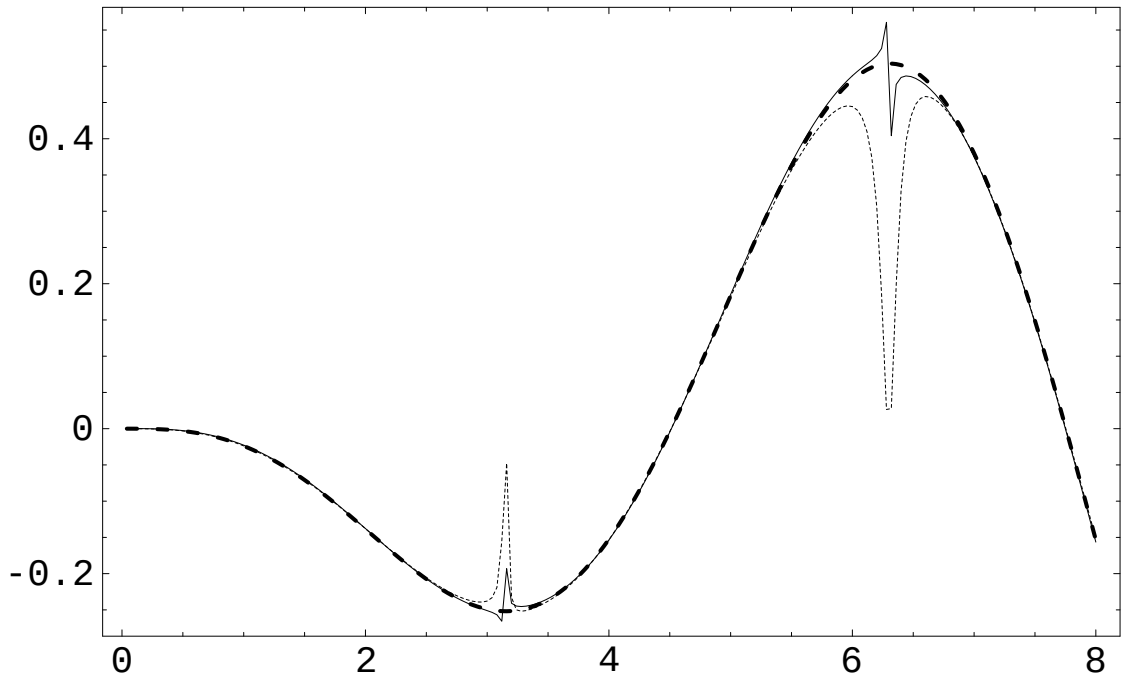

b) Imaginary Part

Figure 4: The course of the solutions in dependence on the wave number - Exterior problem

Finally, we consider the behaviour of the solution using the Fourier method in dependence on the dimension N of the respective interior and exterior problems.
In order to do this we differentiate between the convergence for a fixed wave number κ with the discretisation parameter h tending to 0, and the behaviour of the error for $\kappa h = const.$, cf. [4].
Table 1 shows the convergence of the solutions v_{FT} for $\kappa = \pi/2$.

N	κh	$\|\|v^* - v_{FT}\|\|_{\mathbb{L}_2}$ (interior)	$\|\|v^* - v_{FT}\|\|_{\mathbb{L}_2}$ (exterior)
20	0.953	0.104E-01	0.595E-01
80	0.538	0.459E-02	0.148E-01
320	0.278	0.161E-02	0.873E-02
1280	0.140	0.894E-03	0.674E-02

Table 1: Convergence of the solutions for $\kappa = \pi/2$

The behaviour of the error for various wave numbers satisfying the condition $\kappa h \approx 0.7$ is printed in Table 2.
Notice that the deviation of the solution of the interior problem arises from the fact that the wave number $\kappa = 7.84$ lies close to an eigenvalue of the Laplacian (see also Figure 2).

N	κ	κh	$\|\|v^* - v_{FT}\|\|_{\mathbb{L}_2}$ (interior)	$\|\|v^* - v_{FT}\|\|_{\mathbb{L}_2}$ (exterior)
20	1.15	0.698	0.727E-02	0.566E-01
80	2.04	0.697	0.682E-02	0.145E-01
320	3.94	0.699	0.740E-02	0.222E-01
1280	7.84	0.702	0.122E-01	0.203E-01

Table 2: $\mathbb{L}_2$ error of the solutions for various κ with $\kappa h \approx 0.7$

It should be pointed out that the new scheme uses only half of the computing time compared to the case using standard techniques.

8 Conclusions

In this paper, we presented a new numerical method for the multifrequency analysis of the Helm- holtz equation. We illustrated the advantages of the transformed matrix, which is real and has a sparse structure. Numerical tests of the new procedure show that the agreement of the boundary element results with the analytical solutions is good.

References

[1] C. A. Brebbia, J.C.F. Telles, and L.C. Wrobel, editors. *Boundary element techniques.* Springer-Verlag, Berlin, 1984. Theory and applications in engineering.

[2] G. Chen and J. Zhou. *Boundary element methods.* Academic Press Ltd., London, 1992.

[3] David L. Colton and Rainer Kress. *Integral equation methods in scattering theory.* Krieger Publishing Company, Malabar, 1992.

[4] Klaus Giebermann. *Schnelle Summationsverfahren zur numerischen Lösung von Integral- gleichungen für Streuprobleme im* R^3. Dissertation, Universität Karlsruhe, 1997.

[5] Lars Hoermander. *The analysis of linear partial differential operators, I.* Springer-Verlag, Berlin, second edition, 1990. Distribution theory and Fourier analysis.

[6] Jean-Claude Nédélec. *Acoustic and electromagnetic equations.* Springer-Verlag, New York, 2001. Integral representations for harmonic problems.